Sciencexpress Report

Role of Histone H3 Lysine 9 Methylation in Epigenetic Control of Heterochromatin Assembly

Jun-ichi Nakayama,[1] Judd C. Rice,[2] Brian D. Strahl,[2] C. David Allis,[2] Shiv I. S. Grewal[1]*

[1]Cold Spring Harbor Laboratory, Post Office Box 100, Cold Spring Harbor, NY 11724, USA. [2]Department of Biochemistry and Molecular Genetics, University of Virginia, Charlottesville, VA 22908, USA.

*To whom correspondence should be addressed. E-mail: grewal@cshl.org

The assembly of higher-order chromatin structures has been linked to the covalent modifications of histone tails. We provide in vivo evidence that lysine 9 of histone H3 (H3 Lys9) is preferentially methylated by the Clr4 protein at heterochromatin-associated regions in fission yeast. Both the conserved chromo- and SET domains of Clr4 are required for H3 Lys9 methylation in vivo. Localization of Swi6, a homologue of *Drosophila* HP1, to heterochomatic regions is dependent upon H3 Lys9 methylation. Moreover, an H3 specific deacetylase Clr3 and a β-propeller domain protein Rik1 are required for H3 Lys9 methylation by Clr4 and Swi6 localization. These data define a conserved pathway wherein sequential histone modifications establish a 'histone code' essential for the epigenetic inheritance of heterochromatin assembly.

The organization of the higher-order chromatin structure has been linked to the post-translational modifications of histone tails, including acetylation, phosphorylation and methylation *(1)*. It has been suggested that distinct combinations of covalent histone modifications, also referred to as the 'histone code', provides a 'mark' on the histone tails to recruit downstream chromatin-modifying proteins *(2, 3)*. This is best illustrated by recent studies indicating that the conserved bromodomain of several transcriptional coactivators bind specifically to acetylated lysine residues on histone tails *(4, 5)*. The mechanisms responsible for the establishment and maintenance of multiple covalent modifications within the same or different histone tail are not fully understood.

Modifications of histone tails have also been linked to heterochromatin assembly. Histones H3 and H4 are largely hypoacetylated in heterochromatic chromosomal regions in organisms as diverse as yeast, flies and mammals *(6-8)*. In fission yeast, hypoacetylation of histones is associated with the silent mating-type region and centromeres *(9, 10)*, chromosomal domains that share many parallels with heterochromatic regions in higher eukaryotes *(11)*. Centromeric regions comprising a central core of unique sequences surrounded by inner (*imr)* and outer (*otr*) repeats are assembled into silenced chromatin structures *(12)*. Similarly, a large ~15-kb chromosomal domain at the mating-type (*mat2/3*) region, including the *mat2* and *mat3* loci and an interval between them, known as the *K*-region, is maintained in a silent epigenetic state *(13, 14)*. Among the trans-acting factors that affect silencing at these regions, Clr3 and Clr6 belong to family of histone deacetylases (HDACs) *(15)*. Swi6 and Clr4 proteins contain a chromodomain, an evolutionarily conserved motif initially identified in HP1 and *Polycomb* proteins *(16-18)*. Recently, both Clr4 and its mammalian counterpart, SUV39H1, have been shown to possess intrinsic histone H3-specific methyltransferase (HMTase) activity in vitro *(19)*. However, it is not known whether histones are the physiological targets of these methyltransferases in vivo.

Consistent with previous findings, recombinant Clr4 (rClr4) was found to contain HMTase activity exclusively for histone H3 (Fig. 1B). To identify the specific residue of H3 methylated by rClr4, synthetic peptides derived from the N-terminus of H3 were used as substrates in an in vitro HMTase assay *(20, 21)*. Clr4 preferentially methylated the H3 1-20 unmodified peptide, but failed to methylate the H3 19-35 unmodified peptide (Fig. 1C), indicating that the target residue of Clr4 HMTase resides in the first 20 amino acids of H3. To determine this target residue, a synthetic H3 1-20 peptide set was developed that contained covalent modifications on different amino acids. Using these peptides as substrates, only acetyl- or methyl- modifications on Lys9 effectively blocked rClr4 HMTase activity indicating that Clr4, like its mammalian homologue SUV39H1 *(19)*, selectively methylates Lys9 of H3. Furthermore, similar to SUV39H1, rClr4 HMTase activity was inhibited by phosphorylation of serine 10 (Fig. 1C). These results demonstrate that enzymatic features of the Su(var)3-9 protein family are evolutionarily conserved from yeast to humans.

A recent study demonstrated that the conserved SET domain and two flanking cysteine-rich regions were required for SUV39H1 HMTase activity in vitro *(19)*. To determine whether the conserved domains, the chromo, SET and cysteine-rich regions, were also critical for Clr4 HMTase activity, mutant Clr4 proteins were tested for HMTase activity. While mutations in the chromodomain (W31G and W41G) had little effect on Clr4 HMTase activity, mutations in the SET domain, (G378S) and both cysteine-rich regions (R320H and G486D) greatly reduced Clr4 HMTase activity indicating that these three regions are critical for Clr4 HMTase activity in vitro (Fig. 1A and B).

To test the hypothetical correlation between H3 Lys9 methylation and silencing, an H3 Lys9-methyl specific antibody was developed. In an ELISA, the H3 Lys9-methyl antibody specifically recognized the H3 1-20 Lys9-methyl peptide in a wide range of antibody dilution *(22)*. Moreover, the H3 Lys9-methyl antibody did not detect recombinant histone H3 (rH3) alone compared to the HeLa core histone positive control, but did detect rH3 selectively methylated by rClr4 (Fig. 2A), further demonstrating the specificity of this antibody. Using this antibody in chromatin immunoprecipiation (ChIP) experiments *(10)* (Fig. 2B), it was found that the H3 Lys9-methyl modification is

specifically localized at the silenced chromosomal regions. Interestingly, H3 Lys9 methylation and Swi6 were preferentially enriched at a marker gene (*Kint2::ura4*$^+$) inserted within the silenced *mat2/3* chromosomal domain, compared to control *ura4DS/E* locus at the endogenous location (Fig. 2C). Similarly, H3 Lys9 methylation was also preferentially enriched at the *ura4*$^+$ marker inserted within the highly repressed inner most repeat (*imr1R::ura4*$^+$) and the outer repeat (*otr1R::ura4*$^+$), but not at the weakly repressed central core (*cnt1::ura4*$^+$) of *cen1* (Fig. 2D). In addition, H3 Lys9 methylation coincided with the presence of Swi6 at these regions (Fig. 2D) *(23)*. These findings suggest that H3 Lys9-methyl modification and Swi6 are preferentially localized to silent chromosomal regions and that Swi6 localization is functionally dependent upon H3 Lys9 methylation.

We next sought to determine the biological effect of Clr4 on H3 Lys9 methylation and Swi6 localization at *mat2/3* region and centromeres. Compared to the relatively high levels of Swi6 and H3 Lys9 methylation at both *Kint2::ura4*$^+$ and *otr1R::ura4*$^+$ in wild-type cells, Swi6 and H3 Lys9 methylation were absent in a *clr4*Δ strain at both loci (Fig. 3A and B). This result suggests that H3 Lys9 is the physiological target of Clr4 HMTase activity and that Clr4 appears to be the exclusive in vivo H3 Lys9-specific HMTase at *mat* and *cen* loci. In comparison to our in vitro result showing that only SET domain is required for Clr4 HMTase activity (Fig. 1B), we found that both the chromo- and SET domains are required for H3 Lys9 methylation and Swi6 localization in vivo (Fig. 3C and D). Taken together, these results indicate that the chromodomain is presumably required for targeting Clr4 to the *mat2/3* region and centromeres, while the SET domain and associated cysteine-rich regions of Clr4 constitute the catalytic site.

Remarkably, the Swi6 levels at *mat* and *cen* in different *clr4* mutant backgrounds were directly correlated with H3 Lys9 methylation levels (Fig. 3C and D), further suggesting that Swi6 localization at silent chromosomal domains is functionally dependent on H3 Lys9 methylation. The importance of our in vivo analyses was further highlighted by observations that mutations in Clr4 that decrease its HMTase activity in vitro do not significantly decrease H3 Lys9 methylation and Swi6 localization in vivo. In addition, mutations in the SET domain and the N-terminal cysteine-rich regions of Clr4 (G378S and R320H) greatly reduce H3 Lys9 methylation and Swi6 localization at the *mat* locus, however, these mutations have moderate or negligible effects at *cen1* (Fig. 3C and D). These mutations also have weak effects on centromeric silencing compared to mating-type silencing. Our results are consistent with the notion that enzymatic defects displayed by recombinant monomeric proteins in vitro can be "rescued" by functioning in the context of a multi-subunit complex in vivo. Moreover, the functional organization of the *mat2/3* region and centromeres may differ and that an additional factor(s) may help promote Clr4 activity at centromeres.

Mutations in the *clr3* HDAC, that specifically deacetylates H3 Lys14 *(24)*, affects silencing at *mat* and *cen (12, 15)*. ChIP analysis demonstrated that a *clr3-735* mutant partially defective in H3 Lys14 HDAC activity *(24)* displayed a moderate decrease in H3 Lys9 methylation and Swi6 localization at *otr1::ura4*$^+$ (Fig. 4A), coincident with the apparent reduction in its HDAC activity. This result suggests that H3 Lys14 acetylation inhibits Clr4 HMTase in vivo. To further investigate the functional interaction between Clr3 and Clr4, a double mutant strain was created containing the *clr3-735* and *clr4R320H* mutations, a *clr4* mutation that had the least effect on H3 Lys9 methylation at *otr1R::ura4*$^+$ (Fig. 3D). ChIP analysis of the double mutant demonstrated that H3 Lys9 methylation and Swi6 localization were nearly abolished when compared to the single mutants (Fig. 4A). These findings indicate that Clr3 acts synergistically with Clr4 to effectively localize Swi6 to heterochromatin. In other words, deacetylation of H3 Lys14 by Clr3 is required for H3 Lys9 methylation by Clr4 and for Swi6 localization either indirectly, by altering Clr4 activity, or directly or both. These data also support the theory that residues neighboring Lys9, and potentially their modification states, play a significant role in establishment of the appropriate H3 Lys9-methyl mark.

Previous studies have shown that *rik1*$^+$ affects silencing as well as Swi6 localization at silent loci *(12, 25)*. Computational analyses revealed that Rik1 contains β-propeller domains typically found within WD-40 repeat proteins and are theorized to participate in protein:protein interactions *(26)*. Interestingly, a mutation in *rik1* completely abolished H3 Lys9 methylation and Swi6 localization at both *mat* and *cen* compared to wild type (Fig. 4B). WD-40 proteins are involved in many aspects of chromatin remodeling and histone metabolism, such as chromatin assembly and acetylation or deacetylation of histones *(27)*. Therefore, the β-propeller domains of Rik1 may form a complex with Clr4 to recruit its HMTase activity to heterochromatic regions and may play a role in coupling other trans-acting factors, such as Swi6 and histone deacetylases.

The possible role of Swi6 on Clr4-dependent methylation of H3 Lys9 was also tested. Strains carrying *swi6-115* (W269R) mutation that severely reduced Swi6 protein levels were used. As expected, Swi6 localization at both *mat* and *cen* was abolished as demonstrated by ChIP analysis (Fig. 4C). Interestingly, the *swi6-115* mutation did not cause any detectable change in H3 Lys9 methylation when compared to the wild type strain. These data indicate that Swi6 is dispensable for Clr4 function and suggest that Swi6 acts downstream of Clr4 H3 Lys9 methylation.

Collectively, the above results allow us to define a temporal sequence of events leading to establishment of the silenced chromatin-state with regard to the covalent modifications of the H3 N-terminal tail (Fig. 5). We propose that HDACs and HMTases act cooperatively to establish a 'histone code' that is then recognized by Swi6. More specifically, we propose that the HDACs, Clr6 and/or Hda1, deacetylate H3 Lys9, while Clr3 deacetylates H3 Lys14 prior to H3 Lys9 methylation by the Clr4/Rik1 HMTase complex. Swi6 binding to the H3 Lys9-methyl modification would then result in self-propagating heterochromatin assembly *(10)*. Since the heterochromatin-binding domain of Swi6 was mapped to its chromodomain *(28)*, it is most likely that this protein motif has evolved to recognize the H3 Lys9-methyl modification.

It was recently shown that Swi6 remains associated with the *mat2/3* region throughout the cell cycle where it acts as an important determinant of the epigenetic cellular memory, promoting inheritance of the silenced state *(10)*. Since the mouse homologue of Swi6, M31, associates with Su(var)3-9 *(29)*, a similar interaction between Clr4 and Swi6 is predicted. The close association of Clr4 enzymatic HMTase activity, followed by recruitment and binding of Swi6 to Lys9 methyl 'marks' in H3 via its chromodomain suggest a

pathway of epigenetic inheritance. The extent to which the chromodomain of Clr4 recognizes H3 Lys9-methyl 'marks' is unknown, but it would provide the enzyme a means to bind chromatin as it performs subsequent methylation events. Based on the conservation of Clr4/SUV39H1 and Swi6/HP1 proteins and the presence of H3 Lys9-methyl modification in higher eukaryotes (C.D.A, unpublished; Fig. 2A), we predict that a similar mechanism may be responsible for higher-order chromatin assembly in organisms ranging from fission yeast to humans. Considering the parallels between transcriptional repression by *Polycomb* group proteins in flies and mammals and silencing in fission yeast, it is likely that histone methylation coupled with histone deacetylation may help localize *Polycomb* in pathways that lead to the regulation of homeotic gene expression *(22)*.

References and Notes

1. K. E. van Holde, *Chromatin*, Springer series in molecular biology (Springer-Verlag, New York, 1989).
2. B. D. Strahl, C. D. Allis, *Nature* **403**, 41. (2000).
3. B. M. Turner, *Bioessays* **22**, 836. (2000).
4. C. Dhalluin *et al.*, *Nature* **399**, 491. (1999).
5. R. H. Jacobson, A. G. Ladurner, D. S. King, R. Tjian, *Science* **288**, 1422. (2000).
6. P. Jeppesen, B. M. Turner, *Cell* **74**, 281 (1993).
7. M. Braunstein, A. B. Rose, S. G. Holmes, C. D. Allis, J. R. Broach, *Genes Dev.* **7**, 592 (1993).
8. M. Grunstein, *Cell* **93**, 325. (1998).
9. K. Ekwall, T. Olsson, B. M. Turner, G. Cranston, R. C. Allshire, *Cell* **91**, 1021 (1997).
10. J. Nakayama, A. J. S. Klar, S. I. S. Grewal, *Cell* **101**, 307 (2000).
11. S. I. S. Grewal, *J. Cell Physiol.* **184**, 311 (2000).
12. R. C. Allshire, E. R. Nimmo, K. Ekwall, J. P. Javerzat, G. Cranston, *Genes Dev.* **9**, 218 (1995).
13. S. I. S. Grewal, A. J. S. Klar, *Genetics* **146**, 1221 (1997).
14. G. Thon, A. Cohen, A. J. S. Klar, *Genetics* **138**, 29 (1994).
15. S. I. S. Grewal, M. J. Bonaduce, A. J. S. Klar, *Genetics* **150**, 563 (1998).
16. A. Lorentz, K. Ostermann, O. Fleck, H. Schmidt, *Gene* **143**, 139 (1994).
17. A. V. Ivanova, M. J. Bonaduce, S. V. Ivanov, A. J. S. Klar, *Nat. Genet.* **19**, 192 (1998).
18. J. C. Eissenberg, S. C. Elgin, *Curr. Opin. Genet. Dev.* **10**, 204. (2000).
19. S. Rea *et al.*, *Nature* **406**, 593 (2000).
20. 5 mg of HeLa or chicken core histones were incubated with 0.55 mCi of S-adenosyl-L-[methyl-3H]methionine (3H-AdoMet, 72 Ci/mmol; 1 mM final) and 2 mg of recombinant Clr4 wild type or mutant proteins in 25 ml of HMTase buffer (50 mM Tris, [pH 8.0], 1 mM PMSF, 0.5 mM DTT in 10% glycerol) for 1 hour at 30 ^{o}C. SDS loading buffer was added to half of each sample and boiled followed by separation on a 15% SDS-PAGE gel. The resulting histone bands were visualized by Coomassie staining and fluorography. For the peptide analysis, 5 mg of each peptide derived from the N-terminus of human histone H3 containing a C-terminal cysteine was used. Half of the sample was spotted on Whatman P-81 filter paper, washed 4 times for 10 minutes in 50 mM NaHCO2, [pH 9.0], followed by liquid scintillation counting..
21. B. D. Strahl, R. Ohba, R. G. Cook, C. D. Allis, *Proc. Natl. Acad. Sci. U.S.A.* **96**, 14967 (1999).
22. Supplementary material is available on *Science* online at www.sciencemag.org/cgi/content/full/1060118/DC1.
23. J. F. Partridge, B. Borgstrom, R. C. Allshire, *Genes Dev.* **14**, 783 (2000).
24. J. Nakayama, S. I. S. Grewal and P. Bjerling, K. Ekwall, unpublished data.
25. K. Ekwall *et al.*, *J. Cell Sci.* **109**, 2637 (1996).
26. A. F. Neuwald, A. Poleksic, *Nucleic Acids Res.* **28**, 3570 (2000).
27. A. Verreault, P. D. Kaufman, R. Kobayashi, B. Stillman, *Curr. Biol.* **8**, 96 (1998).
28. G. Wang *et al.*, *Mol. Cell. Biol.* **20**, 6970 (2000).
29. L. Aagaard *et al.*, *EMBO J.* **18**, 1923 (1999).

30. We thank A. Klar, R. Allshire, R. Egel and K. Luger for materials, R. Rice and M. Anne Jelnick for their technical help. This work is funded by grants from Ellison Medical Foundation (S.I.S.G.) and NIH (GM59772 to S.I.S.G. and GM53512 to C.D.A.). J.N. is supported by the HFS fellowship.

22 February 2001; accepted 5 March 2001
Published online 15 March 2001; 10.1126/science.1060118
Include this information when citing this paper.

Fig. 1. Clr4 selectively methylates lysine 9 of histone H3. (**A**) Schematic representation of the Clr4 protein. Conserved domains and locations of the five mutations are shown. (**B**) Effect of mutation in Clr4 on its HMTase activity in vitro. rClr4 wild type and mutant proteins were analyzed in an in vitro HMTase assay using chicken core histones as the substrate and S-adenosyl-[methyl-^{3}H]-methionine as the methyl donor. Samples were separated by 15% SDS-PAGE and visualized by Coomassie staining (bottom). Fluorography indicates the relative HMTase activity of each of the rClr4 proteins (top). The asterisk (*) indicates a histone H3 proteolytic breakdown product. (**C**) rClr4 was used in an in vitro HMTase assay with the following covalently modified peptides from the first 20 amino acids of the N-terminal tail of H3 as substrates: unmodified, dimethylated at lysine 4, dimethylated at lysine 9, acetylated at lysine 9, acetylated at lysine 14 or phosphorylated at serine 10. An unmodified H3 19-35 was also assayed.

Fig. 2. Presence of H3 Lys9 methylation at the *mat* and *cen1*. (**A**) Specificity of the novel H3 Lys9-methyl antibody. Recombinant histone H3 (rH3) was incubated alone or in the presence of rClr4 (rH3+Clr4) in an HMTase assay. The samples, including the HeLa core histone positive control, were separated by SDS-PAGE, transferred to a PVDF membrane and visualized by Ponceau staining (lower). Western blot analysis using the H3 Lys9-methyl antibody is shown (upper). (**B**) DNA isolated from immunoprecipitated chromatin (ChIP) or whole cell extracts (WCE) was quantitatively analyzed using a competitive PCR strategy, whereby one set of primers amplifies a 694 bp and a 426 bp size products from *ura4*$^{+}$ at silenced loci and the control *ura4DS/E* mini-gene at the endogenous location, respectively. PCR fragments were resolved on polyacrylamide gel and then quantified using phosphoimager. (**C**) A physical map of the mating-type locus indicating *Kint2::ura4*$^{+}$ insertion site (upper). Crosshatched box indicates a part of the *K*-region homologous to centromeric repeats. Results from ChIP analysis using the H3 Lys9-methyl or Swi6 antibody are shown. The ratios of *ura4*$^{+}$ and control *ura4DS/E* signals present in WCE were used to calculate relative precipitated

fold enrichment shown underneath each lane. Serial dilution plating assay was used to measure *ura4*$^+$ expression (middle). (**D**) Schematic representation of *cen1* and the corresponding *ura4*$^+$ insertion sites (upper). Levels of H3 Lys9 methylation and Swi6 at the three insertion sites were determined by ChIP analyses (lower). Expression of *ura4*$^+$ markers was assayed using serial dilution plating assay.

Fig. 3. The effect of *clr4* mutations on H3 Lys9 methylation and Swi6 localization at *mat* and *cen1*. (A and B) Deletion of *clr4* abolishes H3 Lys9 methylation and Swi6 localization at *mat* and *cen1*. ChIP analyses were used to compare the levels of H3 Lys9-methyl or Swi6 in wild type or $\Delta clr4$ strains. (C and D) Results from ChIP analyses to determine effect of mutant alleles on H3 Lys9 methylation and Swi6 localization (upper) and silencing phenotypes (lower) are shown. Mutations in *clr4* have varying effects on H3 Lys9 methylation, Swi6 localization and silencing at *Kint2::ura4*$^+$ and *otr1R::ura4*$^+$.

Fig. 4. Functional Clr3 and Rik1, but not Swi6, are required for H3 Lys9 methylation by Clr4. (**A**) Clr3 and Clr4 act synergistically to silence *cen1*. The *clr3-735*, *clr4* $R^{320}H$ and *clr3clr4* double mutant strains were used for ChIP analyses to determine H3 Lys9 methylation and Swi6 localization at *cen1*. (**B**) A *rik1* mutation abolishes H3 Lys9 methylation and Swi6 localization at *mat* and *cen1*. A *rik1-304* mutant strain was used for ChIP analysis to determine H3 Lys9 methylation and Swi6 localization at *mat* or *cen1* loci. (**C**) A *swi6* mutation does not affect Clr4 methylation of H3 Lys9. A *swi6-115* strain was used for ChIP analysis (upper). Western blot analysis using the Swi6 antibody shows Swi6 protein level of wild type or the *swi6-115* mutant strain (lower).

Fig. 5. A step-wise model for heterochromatin assembly leading to epigenetic silencing in *S. pombe*. Green flags and red lollipops represent acetyl- and methyl- modifications, respectively. A nucleosome core particle is comprised of DNA (black line) wrapped around a histone octamer (blue). Orange or green protrusions represent the H3 N-terminal tails with or without acetyl-modifications, respectively.

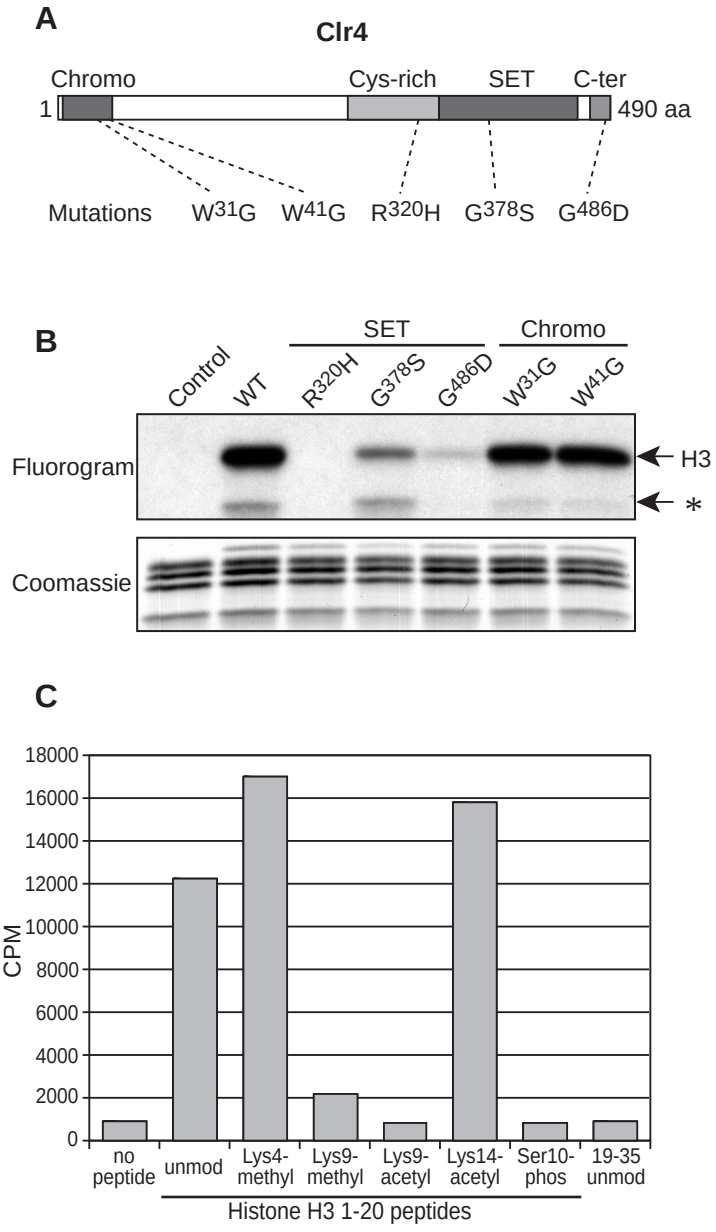

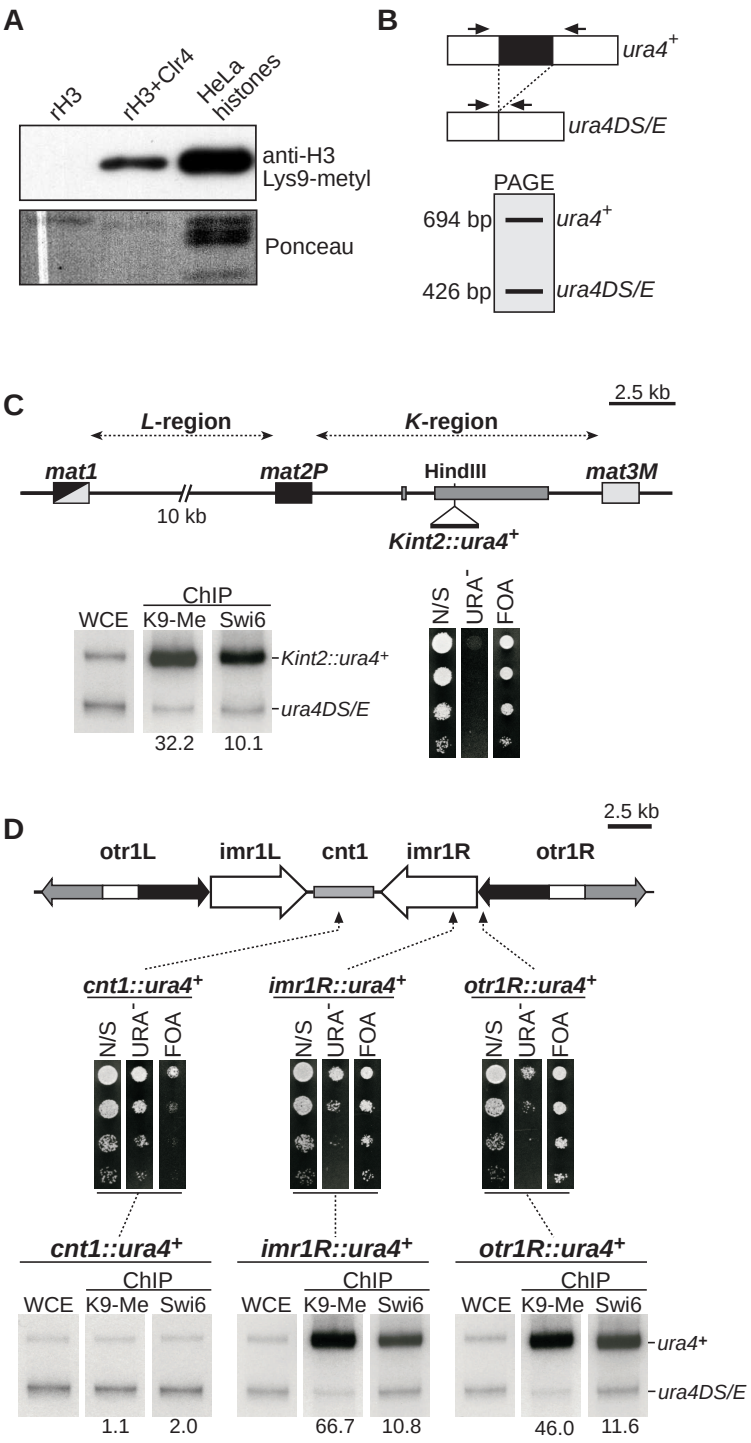

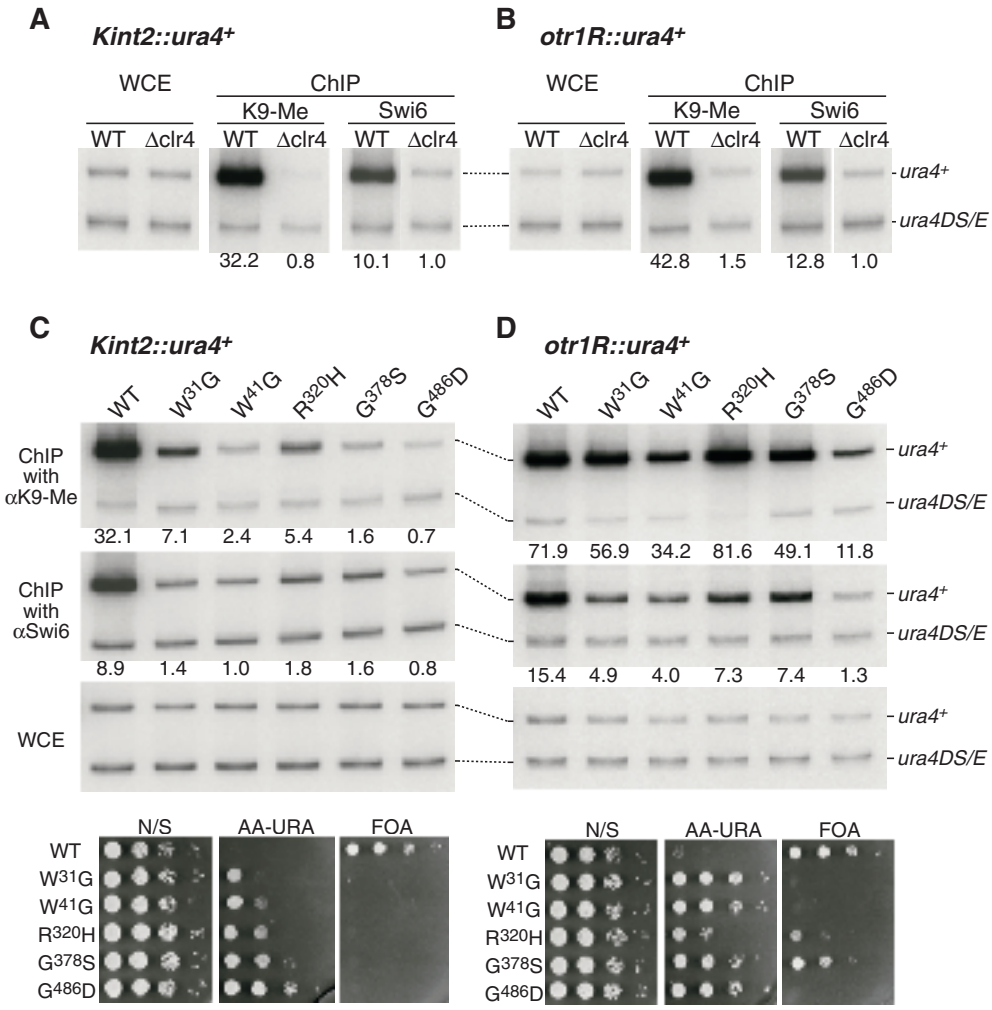
A
Kint2::ura4+
WCE
ChIP
K9-Me
Swi6
WT
Δclr4
32.2
0.8
10.1
1.0
B
otr1R::ura4+
42.8
1.5
12.8
1.0
ura4+
ura4DS/E
C
Kint2::ura4+
WT
W31G
W41G
R320H
G378S
G486D
ChIP with αK9-Me
32.1
7.1
2.4
5.4
1.6
0.7
ChIP with αSwi6
8.9
1.4
1.0
1.8
1.6
0.8
WCE
D
otr1R::ura4+
71.9
56.9
34.2
81.6
49.1
11.8
15.4
4.9
4.0
7.3
7.4
1.3
N/S
AA-URA
FOA